

Quantification of Bone Remodeling in SR μ CT Images of Implants

Hamid Sarve¹, Joakim Lindblad¹, and Carina B. Johansson²

¹ Centre for Image Analysis, Swedish University of Agricultural Sciences
Box 337, 751 05 Uppsala, Sweden
{hamid,joakim}@cb.uu.se

² Department of Clinical Medicine, Örebro University, 701 85 Örebro, Sweden
carina.johansson@oru.se

Abstract. For quantification of bone remodeling around implants, we combine information obtained by two modalities: 2D histological sections imaged in light microscope and 3D synchrotron radiation-based computed microtomography, SR μ CT. In this paper, we present a method for segmenting SR μ CT volumes. The impact of shading artifact at the implant interface is reduced by modeling the artifact. The segmentation is followed by quantitative analysis. To facilitate comparison with existing results, the quantification is performed on a registered 2D slice from the volume, which corresponds to a histological section from the same sample. The quantification involves measurements of bone area and bone-implant contact percentages.

We compare the results obtained by the proposed method on the SR μ CT data with manual measurements on the histological sections and discuss the advantages of including SR μ CT data in the analysis.

1 Introduction

Medical devices, such as bone anchored implants, are becoming increasingly important for the aging population. We aim to improve the understanding of the mechanisms of implant integration. A necessary step for this research field is quantitative analysis of bone tissue around the implant. Traditionally, this analysis is done manually on histologically stained un-decalcified cut and ground sections (10 μ m) with the implant *in situ* (the so called *Exakt* technique [1]). This technique does not permit serial sectioning of bone samples with implant *in situ*. However, it is the state of the art when implant integration in bone tissue are to be evaluated without extracting the device or calcifying the bone. The two latter methods result in interfacial artifacts and the true interface cannot be examined.

The manual assessment is difficult and subjective: these sections are analysed both qualitatively and quantitatively with the aid of a light microscope, which consumes time and money. The desired measurements for the quantitative analysis are explained in Sect. 3.3. In our previous work [2], we present an automated method for segmentation and subsequent quantitative analysis of histological 2D sections. An experience from that work is that variations in staining and various imaging artifacts make automated quantitative analysis very difficult.

Histological staining and subsequent color imaging provide a lot of information, where different dyes attach to different structures of the sample. X-ray imaging and computer tomography (CT) give only grey-scale images, showing the density of each part of the sample. The available information from each image element is much lower, but on the other hand the difficult staining step is avoided and the images, in general, contain significantly less variations than histological images. These last points are crucial, making automatic analysis of CT data a tractable task. In order to widen the analysis and evaluation, we combine the information obtained by the microscope with 3D SR μ CT (synchrotron radiation-based computed microtomography) obtained by imaging the samples before they are cut and histologically stained. Volume data give a much better survey of the tissue surrounding the implant than one slice only. To enable a direct comparison between the two modalities, we have developed a 2D–3D multimodal registration method, presented in [3]. A slice registered according to [3] is shown in Fig. 1a and 1b.

In this work we present a segmentation method for SR μ CT volumes and subsequent automatic quantitative analysis. We compare bone area and bone-implant contact measurements obtained on the 2D sections with the ones obtained on 2D slices extracted from the SR μ CT volumes. In the following section we describe previous work in this field. In Sect. 3.1 the segmentation method is presented. The measurement results from the automatic method are presented in Sect. 4. Finally, in Sect. 5 we discuss the results.

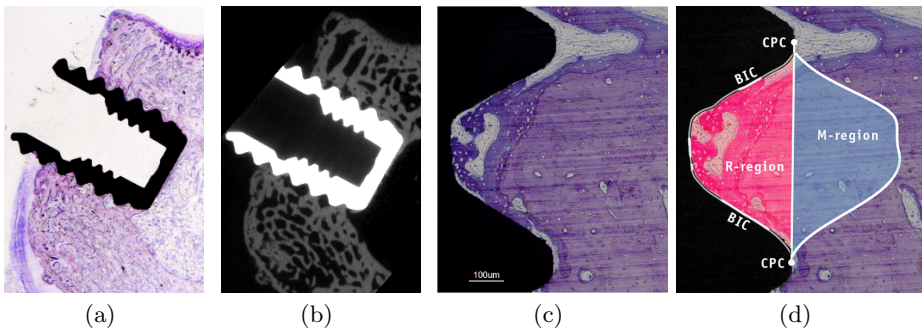


Fig. 1. (a) A histological section (b) Corresponding registered slice extracted from the SR μ CT volume (c) Histological section, single implant thread (d) Regions of interest superimposed on the thread (*CPC*=Center points of the thread crests, *R*-region=the gulf between two *CPC*s and *M*-region=the *R*-region mirrored with respect to the axis connecting two *CPC*s)

2 Background

Segmentation of CT-data is well described in the literature. Commonly used techniques for segmenting X-ray data include various thresholding or region-growing methods. Siverigh and Elliot [4] present a semi-automatic segmentation

method based on connecting pixels with similar intensity. A number of works using thresholding for segmentation of X-ray data are mentioned in [5]. A method for segmentation of CT volumes of bone is proposed by Waarsing et al in [6]. They use local thresholding for segmentation and the result corresponds well to registered histological data.

CT images often suffer from various physics-based artifacts [7]. The causes of these artifacts are usually associated with the physics of the imaging technique, the imaged sample and the particular device used. A way to suppress the impact of such artifacts is to model the effect and to compensate for it [8]. When imaging very dense objects, such as the titanium implants in this study, the very high contrast between the dense object and the surrounding material leads to strong artifacts, that hide a lot of information close to the boundary of the dense object. In this study the regions of interest are close to the boundary of the dense object, which makes imaging of high density implants a very challenging task. When imaging a titanium implant in a standard μ CT device, as can be seen in Fig. 2, a bright aura surrounds the implant region, making reliable discrimination between bone and soft tissue close to the implant virtually impossible.

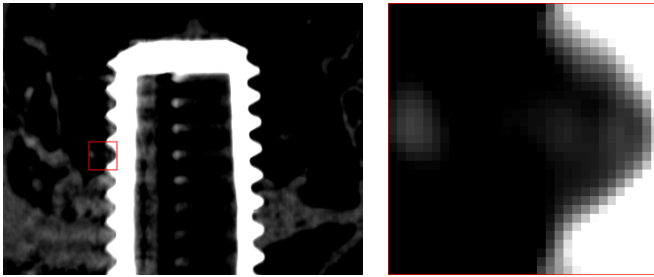


Fig. 2. A titanium implant imaged with a SkyScan1172 μ CT-device. The image to the right is an enlargement of the marked region in the image to left.

3 Material and Methods

Pure titanium screws (diam. 2.2 mm, length 3 mm), inserted in the femur condyle region of twelve-week-old rats for four weeks, are imaged using the SR μ CT device of GKSS (Gesellschaft für Kernenergieverwertung in Schiffbau und Schifffahrt mbH) at HASYLAB, DESY, in Hamburg, Germany, at beamline W2 using a photon energy of 50keV. The tomographic scans are acquired with the axis of rotation placed near the border of the detector, and with 1440 equally stepped radiograms obtained between 0° and 360° . Before reconstruction, combinations of the projection of 0° – 180° and 180° – 360° are built. A filtered back projection algorithm is used to obtain the 3D data of X-ray attenuation for the samples. The field of view of the X-ray detector is set to $6.76\text{mm} \times 4.51\text{mm}$ (width \times height) with a pixel size of $4.40\mu\text{m}$ showing a measured spatial resolution of about $11\mu\text{m}$.

After the SR μ CT-imaging, the samples are divided in the longitudinal direction of the screws. One undecalcified section with the implant *in situ* of 10 μ m is prepared from approximately the mid portion of each sample [9] (see Fig. 1a). The section is routinely stained in a mixture of Toluidine blue and pyronin G, resulting in various shades of purple stained bone tissue and light-blue stained soft tissue components. Finally, samples are imaged in a light-microscope, generating color images with a pixel size of about 9 μ m (see Fig. 1a).

3.1 Segmentation

To reduce noise, the SR μ CT volume is smoothed with a bilateral filter, as described by Smith and Brady [10]. The filter smooths such that voxels are weighted by a Gaussian that extends, not only in the spatial domain, but also in the intensity domain. In this manner, the filter preserves the edges by only smoothing over intensity-homogeneous regions. The Gaussian is defined by the spatial, σ_b , and intensity standard deviation, t .

The segmentation shall classify the volume into three classes; bone tissue, soft tissue and implant. The bone implant is a low-noise high-intensity region in the volume and is easily segmented by thresholding. We use Otsu's method [11], assuming two classes with normal distribution; a tissue class (bone and soft tissue together) and an implant class.

The bone and soft tissue regions, however, are more difficult to distinguish from each other, especially in the regions close to the implant. Due to shading artifacts, the transition from implant to tissue is characterized by a low gradient from high intensity to low (see Fig. 3a). If not taken care of, this artifact leads to misclassifications.

We apply a correction by modeling the artifact and compensate for it. Representative regions with implant-to-bone tissue contact, (IB) and implant-to- soft tissue (IS) are manually extracted. A 3-4 weighted distance transform [12] is computed from the segmented implant region and intensity values are averaged for each distance d from the implant for IB and IS respectively. Based on these values, functions $b(d)$ and $s(d)$ model the intensity depending on the distance d for the two contact types for IB and IS respectively (see Fig. 3c). The corrected image, $I_c \in [0, 1]$, is calculated as:

$$I_c = \frac{I - s(d)}{b(d) - s(d)} \quad \text{for } d > 1. \quad (1)$$

After artifact correction, supervised classification is used for segmenting bone and soft tissue; the respective training regions are marked and their grayscale values are saved. With an assumption of two normally distributed classes, a linear discriminant analysis, LDA, [13] is applied to identify the two classes. To reduce the effect of point noise, an $m \times m \times m$ -neighborhood majority filter is applied on the whole volume after the segmentation.

For $0 < d \leq 1$ however, as seen in Fig. 3c, the intensities of the voxels are not distinguishable and they cannot be correctly classified. The classification of the voxels in this region (to either bone- or soft-tissue) is instead determined by

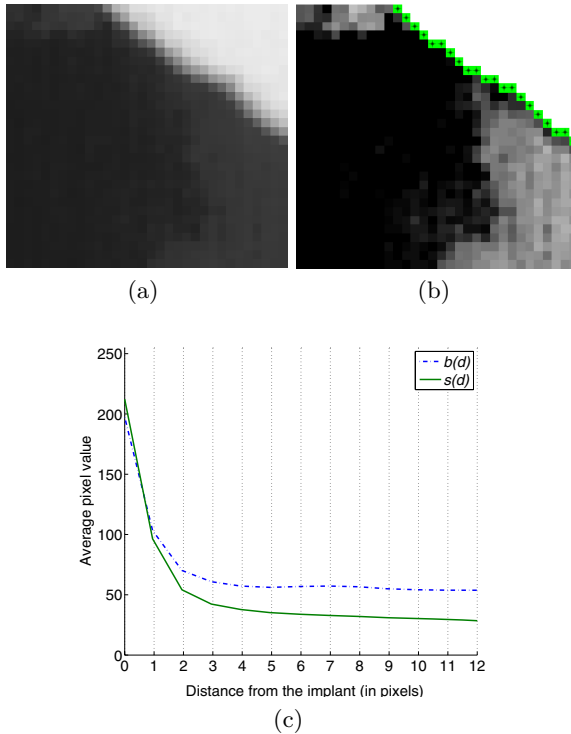


Fig. 3. (a) The implant interface region of a volume slice with implant at upper right (b) Corresponding artifact suppressed region. The marked interface region (stars) cannot be corrected (c) Plot of intensity as a function of distance from the implant for bone, $b(d)$ (dashed) and soft tissue, $s(d)$ (solid line).

the majority filter after the segmentation step. An example of shading artifact correction with the $d = 1$ region marked is shown in Fig. 3b. A segmentation example is shown in Fig. 4.

3.2 Registration

In order to find the 2D slice in the volume that corresponds to the histological section, image registration of these two data types is required. Two GPU-accelerated 2D–3D intermodal rigid-body registration methods are presented in [3]: one based on Simulated Annealing and the other on Chamfer Matching. The latter was used for registration in this work as it was shown to be more reliable. The results show good visual correspondence. In addition to the automatic registration a manual adjustment tool has been added to the method where the user can modify the registration result (six degrees of freedom, three translations and three rotations). After the pre-processing and segmentation of the volume, a slice is extracted using the coordinates found by the registration method. Note that the Chamfer matching used in [3] for registration requires a

segmentation of the implant which is done by using a fixed threshold. The more difficult segmentation into bone and soft tissue is not used in the matching (the other registration approach does not include any segmentation step).

3.3 Quantitative Analysis

The current standard quantitative analysis involves measurements of bone area and bone-implant contact percentages [14]. Fig. 1c shows the regions of interest (ROIs): R =reference, inner area, is measured as the percentage of area covered by bone tissue in the R -region, i.e. the gulf between two center points of the thread crests (CPCs). In addition to R , another bone area percentage, denoted M , is measured as the bone coverage in the region in the gulf mirrored with respect to the axis connecting the two CPCs. A third important measure is BIC , the estimated length of the implant interface where the bone is in contact with the implant, expressed in percentage of the total length of each thread (the gulf between two CPCs).

Area is measured by summing the pixels classified as bone in the R - and M -regions. These regions are found by locating the CPCs (see [2]). BIC -length is estimated using the first of two methods for perimeter estimation of digitized planar shapes presented by Koplowitz and Bruckstein in [15]. This method requires a well defined contour, i.e. each contour-pixel shall have two neighbors only. The implant contour is extracted by dilation with a 3×3 '+'-shaped structural element on the implant region in the segmentation map. The relative overlap between the dilated implant and the bone region is defined as the bone-implant contact. Some post-processing described in [2] is applied to achieve the desired well defined contour.

4 Results

The presented method is tested on a set of five volumes. The parameters for the bilateral filter are set to $\sigma_b = 3$ and $t = 15$ and the neighborhood size of the majority filter is set to $m = 3$. This configuration is empirically assigned and gives a good trade-off between noise-suppression and edge-preservation on the analysed set of volumes. The results of the automatic and manual quantifications are shown in Fig. 5.

Classification of the histological sections is a difficult task and the inter-operator variance can be high for the manual measurements, making a direct comparison with the manual absolute measures unreliable for evaluation purposes; an important manual measurement is the judged relative order of implant integration. Hence, in addition to calculating absolute differences to measure the correspondence between the results of the automatic and manual method, we use a rank correlation technique. The three measures for each thread are ranked for both the proposed and manual method. The differences between the two ranking vectors are stored in a vector \mathbf{d} . Spearman's rank correlation [16],

$$Rs = 1 - \frac{6}{n^3 - n} \sum_{i=1}^n d_i \quad (2)$$

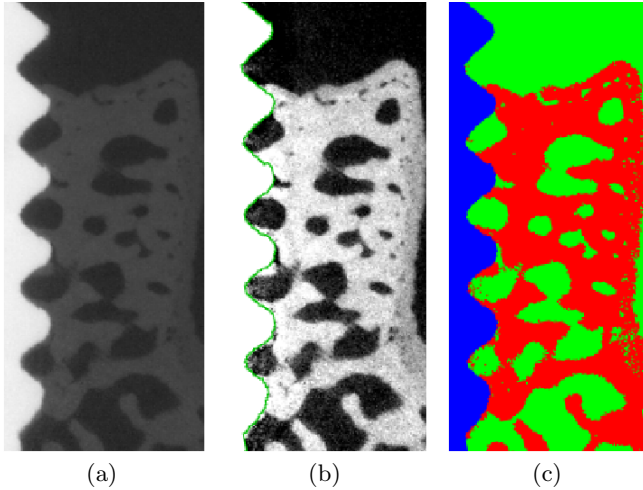


Fig. 4. (a) A slice from the SRμCT volume (b) Artifact corrected slice with the interface region marked and the implant in white to the left (c) A slice from the segmented volume, showing three classes: bone (red), soft tissue (green) and implant (blue)

where n is the number of samples, is utilized for measuring the correlation. A perfect ranking correlation implies $Rs = 1.0$.

The correlation results for all threads for all implant (five implants and ten threads each, 50 threads in total) are presented in Table 1. A two sided t-test shows that we can reject h_0 having probability $P < 0.001$ for all three measures, where h_0 is the hypothesis that the manual and automatic method do not correlate.

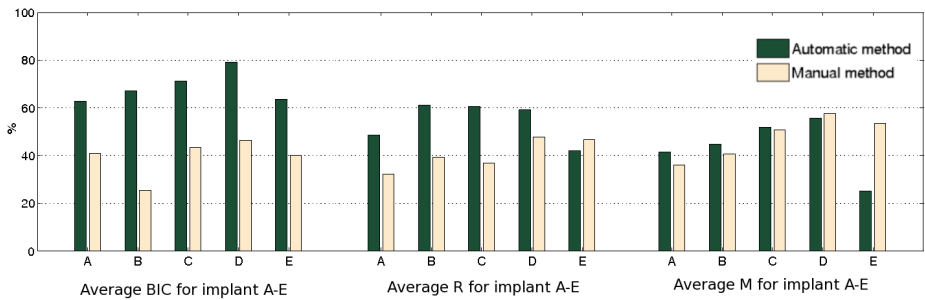


Fig. 5. Averaged absolute values for measures obtained by the automatic and manual method on five implants; the percentage of BIC , R and M averaged over all threads (10 threads per implant)

Table 1. Spearman Rank Correlation, R_s , for ranking of length and area measures (R_{SBIC} , R_{SR} and R_{SM}) for all threads for all implants (50 threads in total)

R_{SBIC}	R_{SR}	R_{SM}
0.5618	0.7740	0.6831

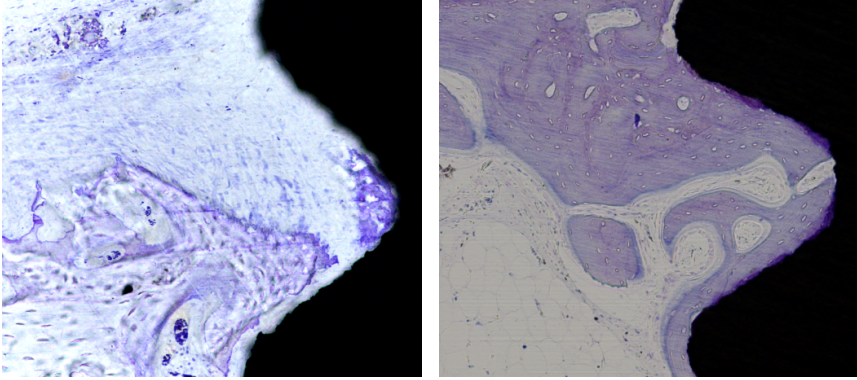


Fig. 6. Two histological sections from two different implants exemplifying variations in tissue structure. The left figure shows more immature bone and more soft tissue regions compared to the right, showing more mature bone.

5 Summary and Discussion

A method for automatic segmentation of SR μ CT volumes of bone implants is presented. It involves modeling and correction of imaging artifacts. A slice is extracted from the segmented volume with the coordinates resulting from a registration of the SR μ CT volume with corresponding 2D histological image. Quantitative analysis (estimation of bone areas and bone-implant-contact percentages) is performed on this slice and the obtained measurements are compared to those obtained by the manual method on the 2D histological slice. The rank correlation shows that the quantitative analysis performed by our method correlates with $R_s = 0.56$ for BIC , $R_s = 0.77$ for R and $R_s = 0.68$ for M . We note that differences between results of the two methods also include any registration errors. Spearman's rank correlation coefficient, shown in Table 1, indicates highly significant correlation ($P < 0.001$) between the automatic ranking, and the manual one. This justifies the use of SR μ CT imaging to perform quantitative analysis of bone implant integration.

The state-of-practice technique of histological sectioning used today reveals information about only a small portion of the sample and the variance of that information is high depending on the cutting position. Furthermore, the outcome of the staining method may differ (as shown in Fig. 6) and the results depend on, e.g., the actual tissue (soft tissue or bone integration), the fixative used, the

section thickness, the biomaterial itself (harder materials in general result more often in shadow effects). Such shortcomings, as well as other types of technical artifacts, make absolute quantifications and automatization very difficult.

SR μ CT-devices require large-scale facilities and cannot be used routinely. The information is limited compared to histological sections, due to lower resolution and grayscale output only. However, the generated 3D volume gives a much broader overview and the problematic staining step is avoided. As shown in Sect. 3.1, the existing artifacts can be removed with satisfactory result and the acquired volumes are similar independent of the tissue type, allowing an absolute quantification.

6 Future Work

Future work involves developing methods for using the 3D data, e.g. estimating bone implant contacts and bone volumes around the whole implant. These measurements will much better represent the entire bone implant integration compared to 2D data. It is also of interest to further extract information from the image intensities, since density variations may indicate differences in the bone quality surrounding the implant.

Acknowledgment

Research technicians Petra Hammarström-Johansson and Ann Albrektsson are greatly acknowledged for skillful sample preparations. Also Dr. Ricardo Bernhardt and Dr. Felix Beckmann are greatly acknowledged. The authors would also like to acknowledge Professor Gunilla Borgfors and Dr. Nataša Sladoje. This work was supported by grants from The Swedish Research Council, 621-2005-3402 and was partly supported by the IA-SFS project RII3-CT-2004-506008 of the Framework Programme 6.

References

1. Donath, K.: Die trenn-dunnschliffe-technik zur herstellung histologischer präparate von nicht schneidbaren gewebe und materialien. *Der Präparator* 34, 197–206 (1988)
2. Sarve, H., et al.: Quantification of Bone Remodeling in the Proximity of Implants. In: Kropatsch, W.G., Kampel, M., Hanbury, A. (eds.) CAIP 2007. LNCS, vol. 4673, pp. 253–260. Springer, Heidelberg (2007)
3. Sarve, H., et al.: Registration of 2D Histological Images of Bone Implants with 3D SR μ CT Volumes. In: Bebis, G., et al. (eds.) ISVC 2008, Part I. LNCS, vol. 5358, pp. 1081–1090. Springer, Heidelberg (2008)
4. Siverigh, G.J., Elliot, P.J.: Interactive region and volume growing for segmenting volumes in mr and ct images. *Med. Informatics* 19, 71–80 (1994)
5. Elmoutaouakkil, A., et al.: Segmentation of Cancellous Bone From High-Resolution Computed Tomography Images: Influence on Trabecular Bone Measurements. *IEEE Trans. on medical imaging* 21 (2002)

6. Waarsing, J.H., Day, J.S., Weinans, H.: An improved segmentation method for in vivo μ CT imaging. *Journal of Bone and Mineral Research* 19 (2004)
7. Barrett, J.F., Keat, N.: Artifacts in CT: Recognition and avoidance. *Radio Graphics* 24, 1679–1691 (2004)
8. Van de Casteele, E., et al.: A model-based correction method for beam hardening in X-Ray microtomography. *Journ. of X-Ray Science and Technology* 12, 43–57 (2004)
9. Johansson, C., Morberg, P.: Cutting directions of bone with biomaterials in situ does influence the outcome of histomorphometrical quantification. *Biomaterials* 16, 1037–1039 (1995)
10. Smith, S., Brady, J.: SUSAN – a new approach to low level image processing. *International Journal of Computer Vision* 23, 45–78 (1997)
11. Otsu, N.: A threshold selection method from gray-level histograms. *IEEE Transactions on Systems, Man, and Cybernetics* 9, 62–66 (1979)
12. Borgefors, G.: Distance transformations in digital images. *Computer Vision, Graphics, and Image Processing* 34, 344–371 (1986)
13. Johnson, R.A., Wichern, D.W.: *Applied Multivariate Statistical Analysis*. Prentice-Hall, Englewood Cliffs (1998)
14. Johansson, C.: On tissue reactions to metal implants. PhD thesis, Department of Biomaterials / Handicap Research, Göteborg University, Sweden (1991)
15. Koplowitz, J., Bruckstein, A.M.: Design of perimeter estimators for digitized planar shapes. *Trans. on PAMI* 11, 611–622 (1989)
16. Spearman, C.: The proof and measurement of association between two things. *The American Journal of Psychology* 100, 447–471 (1987)